PHILOSOPHICAL TRANSACTIONS OF THE ROYAL SOCIETY A MATHEMATICAL, PHYSICAL & ENGINEERING SCIENCES

Optical Diagnostics of Laser-Produced Plasmas with Ultra-Short Laser Pulses

R. Sigel

Phil. Trans. R. Soc. Lond. A 1980 **298**, 407-414
doi: 10.1098/rsta.1980.0263

Phil. Trans. R. Soc. Lond. A **298**, 407–414 (1980)
Printed in Great Britain

Optical diagnostics of laser-produced plasmas with ultra-short laser pulses

By R. Sigel
Projektgruppe für Laserforschung, Max-Planck-Gesellschaft zur Förderung der Wissenschaften e.V., D-8046 Garching bei München, Federal Republic of Germany

In laser fusion experiments the interesting phenomena occur on a picosecond time-scale. Short-pulse lasers in combination with high resolution optics offer a powerful diagnostic tool. After a short description of the principles and experimental techniques I discuss three specific areas of the laser–plasma interaction problem, namely heat transport in the corona of a laser heated pellet, density profile steepening by light pressure and the generation of magnetic fields.

1. Introduction

In laser fusion experiments the phenomena occur on a timescale of picoseconds and a spatial scale of micrometres. Ultra-short laser pulses in combination with high resolution optics can provide the necessary space and time resolution for the investigation of these phenomena.

Now available laser pulses with frequencies in the visible or near u.v. part of the spectrum make it possible to probe the corona of laser-heated pellets. In this zone of the pellet, absorption of the heating laser radiation and transport of the energy to the denser part of the pellet are taking place. At the extremely high fluxes involved, the physical mechanisms of both processes are complicated and still unknown in many respects. Optical diagnostics with ultra-short laser pulses are beginning to contribute to their understanding.

In this short communication I restrict myself to a few specific applications, which are nevertheless representative for the power of the method. I have chosen heat transport in the corona of a laser heated pellet (§3), density profile steepening by light pressure (§4) and the generation of magnetic fields (§5). These sections are preceded by a very brief description of the principles and experimental techniques in §2. The reader who is more deeply interested in either the methods itself or the interaction problems touched in this article is referred to the cited original literature.

2. Principles and experimental techniques

A short laser pulse may be used to probe the corona of a pellet which is heated by an intense laser beam (see figure 1). Propagation of the electromagnetic waves of both the probing and the heating laser is determined by the index of refraction of a plasma

$$\eta^2 = 1-\omega_p^2/\omega^2 = 1-n/n_c.$$

Here $\omega_p=(e^2n/\epsilon_0 m)^{\frac{1}{2}}$ is the plasma frequency, ω the laser frequency and n the electron density. The so-called critical density is defined by $n_c=\omega^2\epsilon_0 m/e^2$, i.e. it is the density where the laser frequency equals the local plasma frequency. From (1), $\eta^2<0$, i.e. η is imaginary for $n>n_c$ (evanescent wave). Thus the radiation can penetrate into the plasma only up to its critical density whereupon it is either reflected or absorbed.

In order that the critical density region of the heating laser may be probed, the wavelength of the probing laser should be markedly shorter than that of the heating laser, otherwise the probing laser beam may be refracted out of the collection angle of the optics. For example, with the Nd^{3+} glass laser as heating laser ($n_c = 10^{21}$ cm^{-3}) and its fourth harmonic as a probe beam ($n_c = 16 \times 10^{21}$ cm^{-3}), the density profile could be measured by interferometry up to $n \approx 2 \times 10^{21}$ cm^{-3}, i.e. twice the critical density of the heating laser. Particularly attractive is the combination of the long-wavelength CO_2 laser ($n_c = 10^{19}$ cm^{-3}), for heating, and a probe laser in the visible range. Densities up to 20 times the critical density of the heating laser could be probed with this combination.

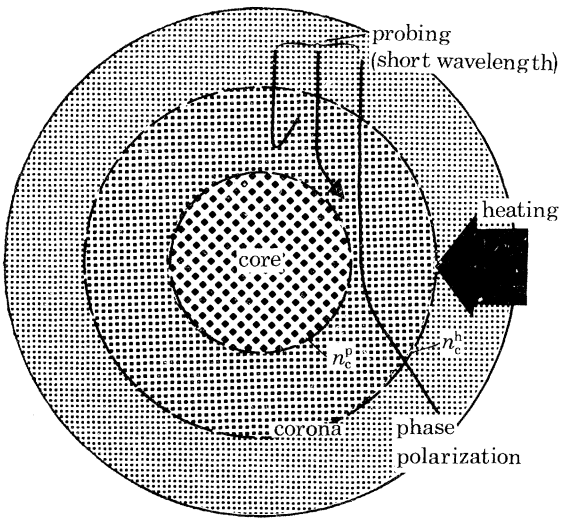

FIGURE 1. Probing of a laser-heated fusion pellet with a shorter wavelength laser; n_c^h and n_c^p are the critical density of the heating and probing laser respectively.

It may be mentioned in passing that probing of the compressed core of the pellet by coherent, ultra-short laser pulses remains a challenging subject for the future. Owing to the high densities aimed at (*ca.* 10^3 times solid state density), this would, however, require pulses in the X-ray region of the spectrum, which are not yet available.

A probe beam may be generated by frequency doubling or quadrupling part of the heating laser beam; actually most of the results presented here have been obtained in this way. This method is, however, not applicable to long wavelength heating (CO_2 laser), where frequency upconversion is difficult to achieve. Furthermore, the probe pulse generated in this manner is not much shorter than the heating pulse and hence time resolution is limited. Laser pulse compression by stimulated Raman backward scattering has been investigated in this context but not yet applied to experiments (Loth & Moy 1979).

More suitable, but also experimentally much more difficult, is the synchronization of a mode-locked probe laser with the heating laser. Both a mode-locked Nd^{3+} glass (Tomov *et al.* 1979) and a ruby (Grek *et al.* 1978) laser were successfully synchronized with a *ca.* 1 ns CO_2 heating pulse. The probe pulse was as short as 20 ps (Grek *et al.* 1978). Mode-locked, flashlamp-pumped dye lasers may also be applied for this purpose (Ariga & Sigel 1976).

The phase shift or the rotation of the polarization of the probe beam after passage through the plasma has been measured to obtain information about the plasma. The phase shift is determined by interferometry; various interferometers, including holographic ones (Attwood *et al.*

1977; Benattar *et al.* 1978; Grek *et al.* 1978; Kohler, D. (cited by Fedosejevs *et al.* 1977*a*); Nomarski 1955).

These interferometers are essentially differential interferometers with a large separation between the two images; interference takes place between the image of the object and an 'empty' part of the field of view. Full use can be made of large-aperture optics with no degrading elements between object and lens since beam splitting in these interferometers takes place after the lens.

Rotation of the polarization of the probe by Faraday rotation may be used to measure magnetic fields in the plasma and is discussed below.

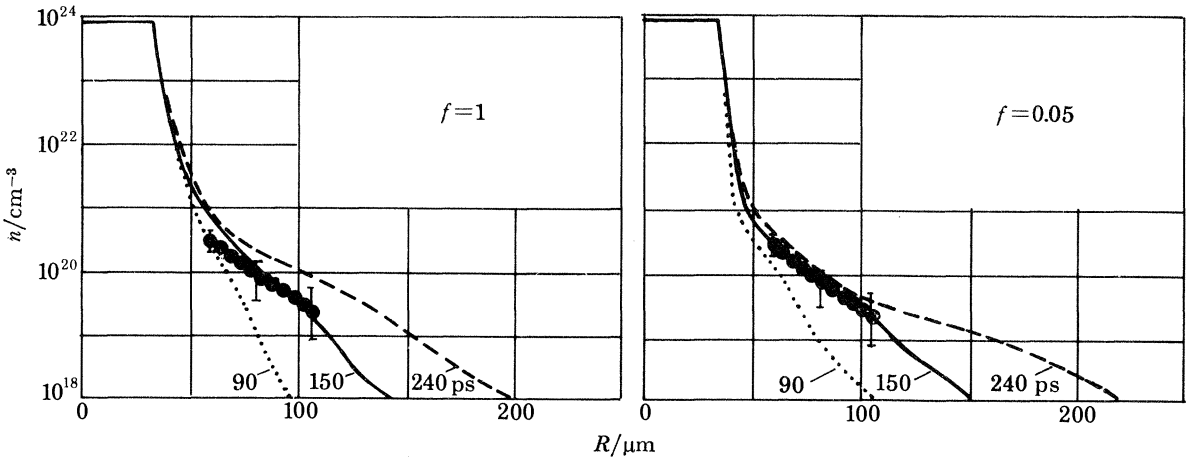

FIGURE 2. Measured and calculated density profiles for a laser irradiated 70 μm diameter glass pellet. The experimental profile has been measured at 150 ps and should be compared with the corresponding curve. Irradiation is with a 100 ps Nd^{3+} glass laser pulse at an average absorbed intensity of 30 TW cm^{-2}. After Benattar *et al.* (1979).

3. HEAT TRANSPORT IN THE CORONA OF A LASER-HEATED PELLET

The absorbed energy is transported away from the absorption region towards the denser part of the pellet by electron heat conductivity. The effectiveness of heat conductivity determines the ablation pressure and is therefore of central importance in the laser-fusion scheme. In the limit of a weak temperature gradient, the electron heat conductivity in a fully ionized plasma has been calculated by Spitzer (1962). This calculation yields the well known temperature-dependent heat flux $S = -\kappa_0 T^{\frac{5}{2}} \partial T/\partial r$.

Experiments, especially measurements of the asymptotic ion expansion velocity (see, for example, Campbell *et al.* 1977), showed, however, that the corona became apparently much hotter than predicted by numerical simulations based on Spitzer heat conductivity. Agreement with experiments could only be obtained if the heat flux in the code was limited by a flux limit factor f to values much below the free streaming limit:

$$|S| = \min\{|\kappa_0 T^{\frac{5}{2}} \partial T/\partial r|; fn(kT)^{\frac{3}{2}}\}.$$

A very hot, rapidly expanding corona due to heat flux limitation should manifest itself also in a flattening of the density profile at subcritical densities. A study of this effect was recently performed at the École Polytechnique (Benattar *et al.* 1979) by time-resolved interferometry of

70 μm diameter glass spheres with the use of a fourth-harmonic probe. Figure 2 shows the measured density profile together with numerically calculated profiles. Agreement is only obtained if considerable flux limitation is assumed ($f \approx 0.05$). Other investigations, entirely different in nature, have implied similar values for f.

Whereas the results thus obtained with the help of ultra-short laser pulses complement very well those obtained by other means, interpretation of the results remains at present a matter of controversy. It is not clear what physical mechanisms of flux limitation have to be attributed to the parameter f. Also, a more detailed picture of heat conductivity must include effects such as the generation of fast electrons during absorption and profile steepening; it has been claimed recently that an alternative interpretation of experiments based on these effects is possible (Gitomer & Henderson 1979). The subject has certainly to await further clarification, both theoretically and experimentally.

4. Density profile steepening due to light pressure

The light pressure of the heating laser may lead to a steepening of the density profile at the critical density. As a consequence, laser light absorption may be strongly modified.

I consider here the case of oblique incidence of a p-polarized electromagnetic wave (i.e. with an electric field component parallel to the density gradient) onto an inhomogeneous plasma. In this case the light pressure is resonantly enhanced owing to coupling with plasma waves and hence may be important even at very low intensities. The coupling is also connected with laser light absorption (Ginzburg 1970). The term 'resonance absorption' is often used in this context.

A very simple model may illustrate the resonant character of the interaction.

Consider a plasma that is inhomogeneous in the x-direction and where the electrons oscillate in the same direction with an amplitude $s(x)$ under the influence of the laser field. In an inhomogeneous plasma this oscillation leads to a space charge and hence an electrostatic field. For small amplitudes one derives readily from Poisson's equation

$$\frac{\partial E}{\partial x} \approx \frac{en}{\epsilon_0}\frac{\partial s}{\partial x}.$$

Integration yields

$$E = ens/\epsilon_0 + E_0 \sin \omega t.$$

Here the driving laser field is simply represented by a homogeneous capacitor field in the x-direction. The equation of motion for the electrons then becomes

$$m\ddot{s} + \omega_p^2(x)\, s = eE_0 \sin \omega t.$$

Resonance occurs for $\omega_p = \omega$, i.e. at the critical density. The energy density connected with the resonant electrostatic field tends to expel the plasma from the resonance region. In an inhomogeneous plasma with flow, this results in the formation of a density step. An analytical treatment in terms of soliton formation has been given by Chen & Liu (1977).

At high laser intensities, light pressure can produce similar effects even without resonant enhancement, i.e. at normal incidence of the laser beam (Lee *et al.* 1977; Mulser & van Kessel 1977; Max & McKee 1977; Virmont *et al.* 1978).

Density profile steepening has now been observed in several laboratories (Fedosejevs *et al.* 1977*b*; Azechi *et al.* 1977; Attwood *et al.* 1978; Raven & Willi 1979). Figure 3 shows a recent

PHILOSOPHICAL TRANSACTIONS OF THE ROYAL SOCIETY A MATHEMATICAL, PHYSICAL & ENGINEERING SCIENCES

result obtained at the Rutherford laboratory (Raven & Willi 1979). A 40 μm diameter glass microballoon was irradiated at 10^{16} W cm^{-2} by a 50 ps Nd^{3+} glass laser pulse. A supercritical ($n \approx 2n_c$) and subcritical ($n \lesssim 0.4\, n_c$) density shelf are connected by a discontinuity whose width was too thin to be resolved in the interferometer (inhomogeneity length $L \lesssim 0.5$ μm).

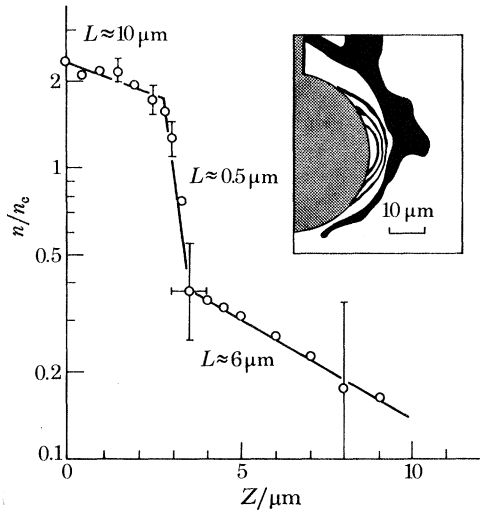

FIGURE 3. Radiation pressure steepened density profile along the laser axis during Nd^{3+} glass laser irradiation at 10^{16} W cm^{-2}. Solid lines are best fits to exponentials of the form exp $(-Z/L)$. The original pellet surface was at $Z = 0$. The inset shows a computer-processed interferogram together with the contours of the 40μm diameter hollow glass microballoon. After Raven & Willi (1979).

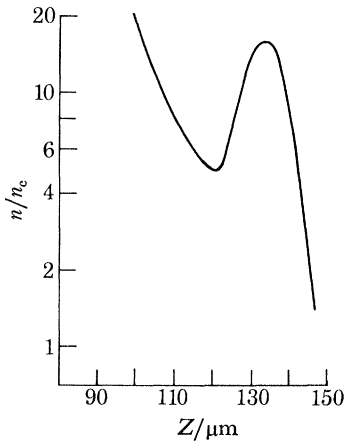

FIGURE 4. Radiation pressure steepened density profile along the laser axis during CO_2 laser irradiation at 7 TW cm^{-2}. The centre of the 144 μm diameter glass microballoon was at $Z = 0$. After Fedosejevs *et al.* (1979).

It should be mentioned in this context that recent absorption measurements have also shown the enhanced absorption ('resonance absorption') for p-polarized light mentioned above (Manes *et al.* 1977; Godwin *et al.* 1977). From the angular dependence of absorption a very steep density gradient $L \approx 1$ μm is derived, in good agreement with the direct observation.

Profile steepening is even more pronounced in the case of CO_2 laser heating (Fedosejevs *et al.* 1977*a*, *b*). Figure 4 shows a recent result of Fedosejevs *et al.* (1979) obtained at the modest

irradiance of 7 TW cm^{-2}. The supercritical shelf density is 15 times the critical density. The upstream density minimum may be due to a compression shock (transition from supersonic to subsonic expansion velocity) as expected theoretically (Virmont *et al.* 1978; Max & McKee 1977). The fine-scale structures observed by Grek *et al.* (1978) make it evident, however, that much remains to be done before these phenomena are completely understood.

Profile steepening has important consequences for the laser–plasma interaction. It is now widely believed that parametric instabilities are largely suppressed by the steep density gradient and are less important for laser light absorption than was orginally thought. Instead, resonance absorption seems responsible for a large fraction of the measured absorption. Also, the very large profile steepening seen with CO_2 laser heating may have the consequence that long wavelength laser heating suffers from the generation of fast electrons to a much lesser extent than was originally thought. This is because for heating in the density jump with its high upper shelf density, many more electrons are available for energy transport than corresponds to the critical density itself. The importance of this result lies in the fact that long wavelength lasers like the CO_2 laser are relatively efficient and are at present the only serious candidates for economic power production by laser fusion.

5. Self-generated magnetic fields

Self-generated magnetic fields in the megagauss range were first observed in plane target irradiation experiments by Stamper & Ripin (1975). They have recently found renewed interest including the case of spherical targets (Stamper *et al.* 1978; Raven *et al.* 1978, 1979). A recent review on this subject has been given by Stamper (1978). Interest in these fields comes from the fact that they may influence energy transport and implosion stability.

Consider a plasma where the electron pressure gradient is balanced by an electric field:

$$enE + \nabla p_e = 0.$$

Together with the equation of state $p_e = nkT$ one eliminates the electric field from Faraday's law and obtains

$$\dot{B} = -\nabla \times E = (k/ne)\nabla T \times \nabla n.$$

Thus whenever ∇T and ∇n are not parallel, a magnetic field will be generated in the plasma.

Experimentally, the magnetic field is measured from the rotation of the polarization of the probe beam (Faraday rotation) and an independent measurement of the line integral of the electron density by interferometry. The technique is described in the article by Stamper (1978).

The experiments with plane targets have shown megagauss fields surrounding the laser axis in a toroidal manner. This is consistent with the temperature gradient cylindrically in toward the laser axis and the density gradient into the target. A recent result obtained at the Rutherford laboratory is shown in figure 5.

At high density, the profile shows a hollowing to a half width equal to the focal spot radius; this is believed to be due to the radiation pressure of the incident laser radiation of 10^{16} W cm^{-2}. In the lower density plasma this changes to a double hollow structure with minima off-axis at the focal spot radius. This correlates well with the position of the toroidal magnetic field. The field pressure in this low-density region can be estimated at approximately 50% of the thermal pressure of the plasma, in agreement with the observed 50% depletion of the local plasma

PHILOSOPHICAL TRANSACTIONS OF THE ROYAL SOCIETY A MATHEMATICAL, PHYSICAL & ENGINEERING SCIENCES

density. The field structure is in general agreement with numerical simulations (Colombant & Winsor 1977).

In a truly spherical situation, magnetic fields should not be generated since ∇T and ∇n are parallel. Experiments with one-sided illumination of spherical pellets have shown strong magnetic fields only if either a pre-pulse was used (Stamper *et al.* 1978) or the focal spot was much smaller than the pellet diameter (Raven *et al.* 1979). Though more detailed investigations are clearly needed, these experiments give hope that disastrous magnetic fields may not occur in spherical, laser-driven implosions.

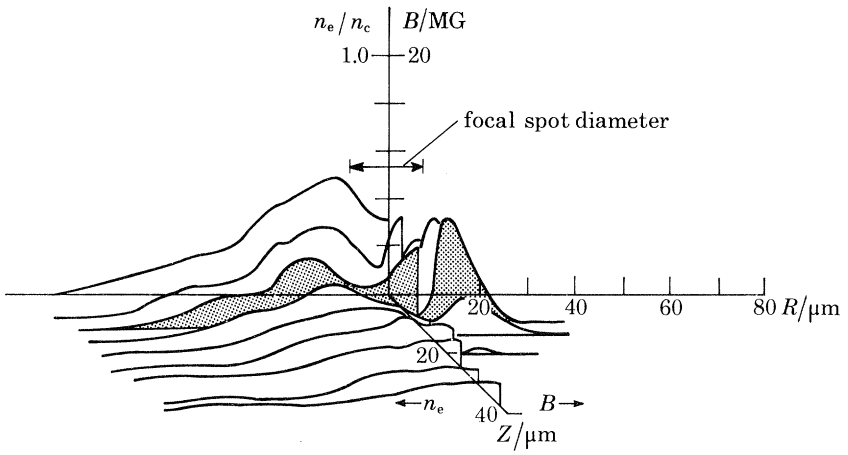

FIGURE 5. Electron density (left) and magnetic field (right) profiles in front of a plane, laser-irradiated target. The Nd^{3+} glass laser beam arrived along the z-axis (axis of rotation symmetry). Irradiance is 10^{16} W cm^{-2} at a focal spot diameter of 15 μm. For the sake of clarity the profiles located at $Z = 10$ μm (target surface at $z = 0$) are enhanced in grey. This plane contains the maximum of the toroidal magnetic field; this maximum coincides with a minimum in density (left-hand side). After Raven & Willi (1979).

I should like to thank D. T. Attwood, A. Raven, M. C. Richardson and J. A. Stamper for their help with original slides for the oral presentation. I am particularly grateful to A. Raven, M. C. Richardson and their collaborators for the allowance to reproduce recent results before publication. Part of the work mentioned in this article was performed at École Polytechnique – GRECO during a time that the author was supported by a C.N.R.S. grant; I should like to thank E. Fabre and his group for their hospitality.

REFERENCES (Sigel)

Ariga, S. & Sigel, R. 1976 *Z. Naturf.* **31a**, 697–706.
Attwood, D. T., Coleman, L. W. & Sweeney, D. W. 1975 *Appl. Phys. Lett.* **26**, 616–618.
Attwood, D. T., Sweeney, D. W., Auerbach, J. M. & Lee, P. H. Y. 1978 *Phys. Rev. Lett.* **40**, 184–187.
Azechi, H., Oda, S., Tanaka, K., Norimatsu, T., Sasaki, T., Yamanaka, T. & Yamanaka, C. 1977 *Phys. Rev. Lett.* **39**, 1144–1147.
Benattar, R., Popovics, C. & Sigel, R. 1979 *Rev. scient. Instrum.* **50**, 1583–1585.
Benattar, R., Popovics, C., Sigel, R. & Virmont, J. 1979 *Phys. Rev. Lett.* **42**, 766–769.
Campbell, P. M., Johnson, R. R., Mayer, F. J., Powers, L. V. & Slater, D. C. 1977 *Phys. Rev. Lett.* **39**, 274–277.
Chen, H.-H. & Liu, Ch.-S. 1977 *Phys. Rev. Lett.* **39**, 1147–1150.
Colombant, D. G. & Winsor, N. K. 1977 *Phys. Rev. Lett.* **38**, 697–701.
Fedosejevs, R., Tomov, I. V., Burnett, N. H. & Richardson, M. C. 1977*a* In *Proc. 12th Int. Congr. High Speed Photography* (*Photonics*) (vol. 97 of *High speed photography*) (Toronto 1976) (ed. M. C. Richardson), pp. 401–406. Bellingham: S.P.I.E.

Fedosejevs, R., Tomov, I. V., Burnett, N. H., Enright, G. D. & Richardson, M. C. 1977*b* *Phys. Rev. Lett.* **39**, 932–935.
Fedosejevs, R., Burgess, M. D. J., Enright, G. D. & Richardson, M. C. 1979 Presented at 9th Annual Conference on Anomalous Absorption of Electromagnetic Waves. Rochester, New York.
Ginzburg, V. L. 1970 *The propagation of electromagnetic waves in plasmas*, 2nd ed, p. 260. Pergamon.
Gitomer, S. J. & Henderson, D. B. 1979 *Physics Fluids* **22**, 364–366.
Godwin, R. P., Sachsenmaier, P. & Sigel, R. 1977 *Phys. Rev. Lett.* **39**, 1198–1201.
Grek, B., Martin, F., Johnston, T. W., Pépin, H., Mitchel, G. & Rheault, F. 1978 *Phys. Rev. Lett.* **41**, 1811–1814.
Lee, K., Forslund, D. W., Kindel, J. M. & Lindman, E. L. 1977 *Physics Fluids* **20**, 51–54.
Loth, C. & Moy, J. P. 1979 *Optics Commun.* **28**, 365–368.
Manes, K. R., Rupert, V. C., Auerbach, J. M., Lee, P. & Swain, J. E. 1977 *Phys. Rev. Lett.* **39**, 281–284.
Max, C. E. & McKee, C. F. 1977 *Phys. Rev. Lett.* **39**, 1336–1339.
Mulser, P. & van Kessel, C. 1977 *Phys. Rev. Lett.* **38**, 902–905.
Nomarski, M. G. 1955 *J. Phys. Radium* **16**, 9S.
Raven, A., Willi, O. & Rumsby, P. T. 1978 *Phys. Rev. Lett.* **41**, 554–557.
Raven, A., Rumsby, P. T., Stamper, J. A., Willi, O., Illingworth, R. & Thareja, R. 1979 *Appl. Phys. Lett.* **35**, 526–529.
Raven, A. & Willi, O. 1979 *Phys. Rev. Lett.* **43**, 278–281.
Sigel, R. 1969 *Phys. Lett.* A **30**, 103–104.
Spitzer Jr, L. 1962 *Physics of fully ionized gases*. John Wiley.
Stamper, J. A. & Ripin, B. H. 1975 *Phys. Rev. Lett.* **34**, 138–141.
Stamper, J. A., McLean, E. A. & Ripin, B. H. 1978 *Phys. Rev. Lett.* **40**, 1177–1181.
Stamper, J. A. 1978 *A perspective on self-generated magnetic fields*. N.R.L. memorandum report no. 3872.
Tomov, I. V., Fedosejevs, R. & Richardson, M. C. 1979 *Rev. scient. Instrum.* **50**, 9–16.
Virmont, J., Pellat, R. & Mora, P. 1978 *Physics Fluids* **21**, 567–573.

PHILOSOPHICAL TRANSACTIONS OF THE ROYAL SOCIETY A MATHEMATICAL, PHYSICAL & ENGINEERING SCIENCES